6. V. E. Minashin, A. A. Sholokhov, and Yu. I. Gribanov, Thermophysics of Liquid-Metal-Cooled Nuclear Reactors [in Russian], Atomizdat, Moscow (1971).
7. Rau, Teploperedacha, 95, No. 2, 67 (1973).
8. Roidt et al., Teploperedacha, 96, No. 2, 61 (1974).
9. Lund, Teploperedacha, 98, No. 1, 17 (1976).
10. Karadzhileskov and Todreas, Teploperedacha, 98, No. 2, 125 (1976).
11. P. A. Ushakov, in: Proceedings of the Power Physics Institute [in Russian], Atomizdat, Moscow (1974), p. 263.
12. W. A. Sutherland, Heat Transfer in Rod Bundles, ASME, New York (1968), pp. 104.

DESIGN OF A HEAT PIPE WITH SEPARATE CHANNELS FOR VAPOR AND LIQUID

Yu. E. Dolgirev, Yu. F. Gerasimov, Yu. F. Maidanik, and V. M. Kiseev

UDC 621.565.58(088.8)

The design of a limited rate heat pipe with individual channels for vapor and liquid is discussed.

One of the efficient structures for low-temperature heat pipes to transmit heat in the direction of the gravity field is the heat pipe with separate channels for vapor and liquid — the antigravity heat pipe (AGHP) [1, 2]. The complexity of the physical processes occurring in this type of heat pipe has been an obstacle to a rigorous analytical description of its operation.

In this paper we describe the calculation of the heat-transfer capability and definition of the conditions of operation of an AGHP operating in the evaporation regime (Fig. 1). The input data for the design are the "height" of the heat pipe, its geometrical dimensions, the characteristics of the capillary-porous structure, and also the temperatures of the vapor and condensate being supplied. In the calculation we define the maximum allowable heat-flux surface density in the evaporator and the wall temperature of the compensating cavity, and we verify the condition for boiling of liquid in the cavity.

Under the limiting heat load the capillary heat is equal to the sum of the pressure drops in the individual sections of the heat pipe. The basic equation for a heat pipe of this construction has the form

$$Q\frac{128\eta''L_{ve}}{\pi l\rho'' d_{ve}^4 n_{ve}} + Q^2\frac{8\Lambda L_{vc}}{\pi^2 l^2\rho'' d_{vc}^5} + Q\frac{128\eta' L_{lc}}{\pi l\rho' d_{lc}^4} + Q\frac{a}{\Pi r_p^2}\frac{\eta'}{2\pi l\rho' L_{ve}}\left(\ln\frac{R_2}{R_1} + 2\ln\frac{R_2+d_{ve}}{R_2} + \frac{\pi d_{ve}}{(R_3-R_2-d_{ve})n_{ve}}\right) + \rho' gL\sin\varphi = \frac{\xi\sigma\cos\theta}{r_p}. \quad (1)$$

The first term on the left-hand side of Eq. (1) is the pressure drop in the vapor channels of the evaporator; the second term is the drop in the main vapor channel; the third term is the drop in the liquid channel; the fourth term is the friction loss during motion of liquid along the support wall of the wick; the fifth term is the same for the motion of the liquid through the contractions between the vapor channels of the evaporator; and the sixth term is the loss in the wall layer of the evaporator. The complex geometry of the last two sections in this design is approximated by a simpler structure. The wick section from R_2 to $R_2 + d_{ve}$ between the vapor-emission channels is approximated by an annular layer with the same radii. Contraction of the section carrying liquid is taken into account by an appropriate coefficient (in this case equal to 2), which is obtained by optimizing the number of vapor-emission channels. The wall section for each vapor-emission channel is approximated by a rectangular section with an average length equal to d_{ve} and an average width of $R_3 - R_2 - d_{ve}$, equal to the thickness of the wall layer. The quantity $\Pi r_p^2/a$ is the perme-

S. M. Kirov Ural Polytechnic Institute, Sverdlovsk. Translated from Inzhenerno-Fizicheskii Zhurnal, Vol. 34, No. 6, pp. 988-993, June, 1978. Original article submitted January 28, 1977.

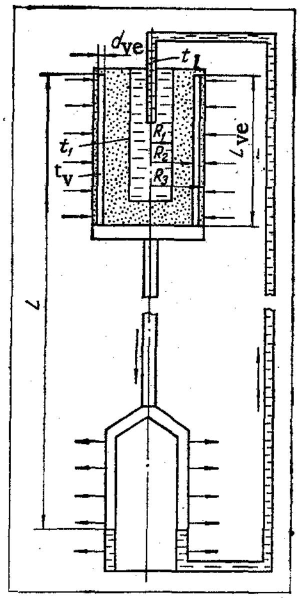

Fig. 1. Schematic of the heat pipe.

ability coefficient. The seventh term is the pressure drop due to the hydrostatic column of liquid.

In setting up equation (1) we allowed for the fact that the most intense evaporation occurs from the surface of the vapor-emission channels, located close to the outside wall of the evaporator.

During operation of the heat pipe with any heat-transfer agent, over a wide range of power transfer, including the limiting values, laminar flow conditions are achieved for the heat-transfer agent in all the sections, i.e., the condition

$$\mathrm{Re} = \frac{4Q}{\pi l \eta d n} < \mathrm{Re}_{cr},$$

is satisfied; here d, n, and η are the diameter, the number of parallel channels, and the viscosity of the heat-transfer agent at a given section, and Re_{cr} is the critical Reynolds number, equal to 2300.

An exception is the main vapor channel, in which turbulent vapor flow conditions occur because of its small diameter. The vapor-channel diameter in an AGHP is limited by the condition that the compensation cavity volume should be equal to the sum of the volumes of the vapor channel and the condenser. The resistance coefficient is calculated from experimental data.

In contracted form, Eq. (1) can be written as

$$AQ^2 + BQ + \frac{a}{\Pi r_p^2} DQ + \rho' g L \sin\varphi = \frac{\xi\sigma\cos\theta}{r_p}, \tag{2}$$

where A, B, and D are, respectively, parametric groups in Q^2 and Q. From Eq. (2) we can determine Q:

$$Q = \sqrt{\left(\frac{B}{2A} + \frac{Da}{2A\Pi r_p^2}\right)^2 + \frac{\xi\sigma\cos\theta}{Ar_p} - \frac{\rho' g L \sin\varphi}{A}} - \left(\frac{B}{2A} + \frac{Da}{2A\Pi r_p^2}\right). \tag{3}$$

The heat flux transmitted by the pipe depends on the radius of the pores. It will be a maximum for a specific optimal pore radius.

By applying the usual procedure for finding an extremum of $\partial Q/\partial r_p$, we can determine the optimal pore radius r_{opt} corresponding to a given pipe geometry, its operating height, and a given heat-transfer agent. An accurate value of r_{opt} is calculated by a computer. The characteristic form of curves calculated from Eq. (3), i.e., the dependence of transferred power

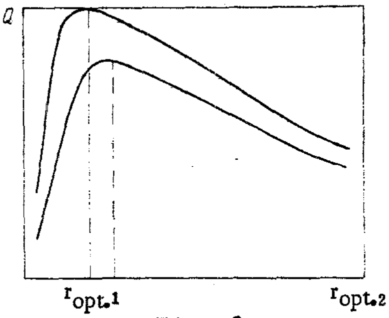

Fig. 2

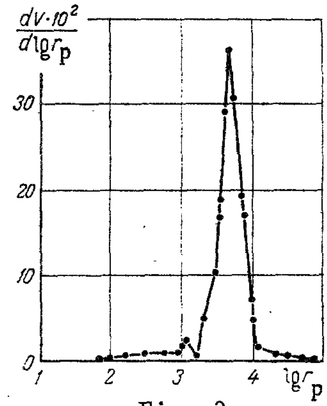

Fig. 3

Fig. 2. Characteristic shape of curves calculated from Eq. (3), $\Pi_1 > \Pi_2$.

Fig. 3. Differential curve for distribution of pore volume with respect to radius: r_p is the radius of the pores, Å.

on pore radius for wicks with various porosities, is presented in Fig. 2, from which one can see that an increase in wick porosity leads to an increase in Q, which leads, in turn, to an increase in the friction loss in the outer circuit, this, correspondingly, leading to a reduction in the optimal pore radius. The values of Q obtained were calculated for an ideal wick, in which all the pores have the same radius, equal to the optimal value. In actual porous bodies there is a distribution of pore radius. Each pore radius has its own permeability, a dynamic quantity which determines a set of pores with a range of variation from a given radius downward. It can be determined as follows:

$$K_m = \sum_{i=1}^{m} K_i = \sum_{i=1}^{m} \frac{\Delta\Pi_i r_{pi}^2}{16}, \tag{4}$$

where K_i, $\Delta\Pi_i$ are the permeability and porosity of the wick for pores of radius from r_{pi-1} to r_{pi}. Equation (4) was obtained from the Poiseuille and Darcy formulas, taking into account that the sinuosity of the capillaries is 2 [3].

The maximum heat flux of a pipe with an actual capillary-porous structure corresponds to the largest term in a series, each of which is calculated from the equation

$$Q_m = \sqrt{\left(\frac{B}{2A} + \frac{D}{2AK_m}\right)^2 + \frac{\xi\sigma\cos\theta}{Ar_{p\,m}} - \frac{\rho' gL\sin\varphi}{A}} - \left(\frac{B}{2A} + \frac{D}{2AK_m}\right). \tag{5}$$

The maximum energy-flux density at the external surface of the evaporator is $q = Q/S$.

For start-up and operation of an AGHP with a given heat-transfer agent and given temperature level, a specific temperature drop at the wick support wall, as well as a corresponding pressure drop from the vapor channel and part of the condenser to the compensation cavity, which must be overcome by the liquid and therefore by the wick feed, is necessary. In addition, the liquid temperature and pressure at the wall of the compensation cavity must correspond to a stable state, i.e., the liquid in this region should not be superheated. If the liquid is in a metastable state, then it may become super-boiled in the compensation cavity. This perturbs the normal wick supply, causes an increase in the vapor temperature, and can lead to the operation of the heat pipe being shut down.

The temperature drop in the wick support wall depends on the wall thickness, the effective thermal conductivity of the wick, the specific heat of the liquid, the vapor temperature, the temperature of the liquid arriving in the compensation cavity, and the liquid flow density in the wick.

The temperature drop at the wick wall can be determined as follows. First we find the temperature distribution in the wick under given boundary conditions, and then the temperature distribution in the liquid occupying the compensation cavity. By matching the solution at the point R_1, we can find the liquid temperature, equal to the temperature of the wick housing at the compensation cavity wall.

The differential equation for energy transfer in a capillary-porous structure filled with liquid which flows counter to the heat flux has the form (in a cylindrical coordinate system) [4]

$$\frac{d^2t}{dr^2}+\frac{1}{r}(1-\varepsilon)\frac{dt}{dr}=0, \tag{6}$$

where $\varepsilon = QC'_p/2\pi l L_{ve}\lambda$.

With the boundary conditions

$$r=R_1 \quad t=t_1;\ r=R_2 \quad t=t_V$$

the solution of Eq. (6) can be written in the form

$$t=t_1+\frac{(t_V-t_1)(r^{\varepsilon}-R_1^{\varepsilon})}{R_2^{\varepsilon}-R_1^{\varepsilon}}. \tag{7}$$

The differential equation for the energy transfer in the liquid filling the compensation cavity has the analogous form

$$\frac{d^2t}{dr^2}+\frac{1}{r}(1-\varepsilon_1)\frac{dt}{dr}=0, \tag{8}$$

where $\varepsilon_1 = QC'_p/2\pi l L_{ve}\lambda'$.

The solution of Eq. (8) with boundary conditions

$$r=0 \ t=t_l;\ r=R_1 \quad \lambda'\frac{dt}{dr}=\lambda_e\frac{dt}{dr}$$

has the form

$$t=t_l+\frac{(t_V-t_1)R_1^{\varepsilon}r^{\varepsilon_1}}{(R_2^{\varepsilon}-R_1^{\varepsilon})R_1^{\varepsilon_1}}. \tag{9}$$

From Eq. (7) and (9) with $r = R_1$ we can find the temperature t_1 at the wall:

$$t_1=\left[t_l+t_V\frac{R_1^{\varepsilon}}{R_2^{\varepsilon}-R_1^{\varepsilon}}\right]\Big/\left[1+\frac{R_1^{\varepsilon}}{R_2^{\varepsilon}-R_1^{\varepsilon}}\right].$$

The temperature drop at the wick support wall for the given operating parameters is $\Delta t = t_V - t_1$.

The main condition for operation of an AGHP is the no-boiling condition for the liquid in the compensation cavity (or, more accurately, at the interface between the liquid–wick regions). This condition may be written as follows:

$$\frac{dP}{dT}(t_V-t_1)\geqslant \Sigma\Delta P, \tag{10}$$

where $\Sigma\Delta P = \Delta P_{ve} + \Delta P_{vc} + \Delta P_{lc} + \Delta P_g$ is the sum of the pressure losses in the outer AGHP circuit; $dP/dT = l\rho'\rho''/T_V(\rho' - \rho'')$ is the tangent of the angle of slope of the saturation line for the heat-transfer agent at a given temperature level of the heat pipe.

It can be seen from Eq. (10) that operation of the AGHP depends on the temperature level at which it operates, on the curvature of the saturation line of the given heat-transfer agent, and also on the hydraulic resistance of the outer circuit.

Table 1 shows the results of calculations carried out for a single heat pipe, charged with various heat-transfer agents, and with the following geometric dimensions: $L_{ve} = 7\cdot10\ m^{-2}$; $d_{ve} = 2\cdot10^{-3}$ m; $n_{ve} = 22$; $L_{ve} = 0.75$ m; $d_{vc} = 5.8\cdot10^{-3}$ m; $L_{lc} = 1.0$ m; $d_{lc} = 3.5\cdot10^{-3}$ m; $L = 0.9$ m; $R_1 = 4\cdot10^{-3}$ m; $R_2 = 11\cdot10^{-3}$ m; $R_3 = 14\cdot10^{-3}$ m.

A wick with $\Pi = 60\%$ was made of electrolytic nickel powder. The differential curve for the distribution of pore volume with respect to radius was taken on a mercury porometer and is shown for this wick in Fig. 3. The total permeability of this wick, computed from Eq. (4), is $K = 1.26\cdot10^{-14}\ m^2$.

TABLE 1. Results of Heat-Pipe Calculation

Heat-transfer agent	Oper. param.			Results of calculations					Exp. data
				ideal wick		actual wick			
	φ, deg	t_v, °C	t_l, °C	r_{opt}, μm	$q \cdot 10^{-4}$, W/m²	r_p, μm	$q \cdot 10^{-4}$, W/m²	condition (10)	$q \cdot 10^{-4}$, W/m²
Acetone	0			1,84	11,01	0,93	4,02	Fulfilled	—
	30	38	25	1,66	9,84	0,91	3,70	"	3,89
	90			1,48	8,53	0,90	3,38	Not fulfilled	3,30
Freon-11	0			3,60	7,65	0,95	1,49	Fulfilled	1,28
	30	40	25	2,00	4,24	0,90	1,21	"	1,08
	90			1,16	2,59	0,86	0,94	Not fulfilled	1,02
Ammonia	0			3,12	61,46	0,95	13,78	Fulfilled	—
	30	35	33	2,68	53,20	0,93	12,93	"	—
	90			2,28	45,05	0,91	12,08	"	—

Table 1 also presents experimental data with acetone and Freon-11, which show good agreement with the results of calculation.

The liquid flux density with acetone and Freon-11 at $\varphi = 90°$ and the given temperatures does not provide the required temperature drop at the wick support wall, i.e., there may be boiling of liquid in the compensation cavity. In this case one observes experimentally an increase in the vapor temperature and a shift in the working point upward along the saturation line to the required temperature level.

NOTATION

L_{ve}, d_{ve}, n_{ve}, length, diameter, and number of the vapor-emission channels of the evaporator; L_{vc}, d_{vc}, length and diameter of the main vapor channel; L_{lc}, d_{lc}, length and diameter of the liquid channel; L, heat-transfer length; S, outer surface area of the evaporator; g, acceleration of gravity; φ, angle between the heat-pipe axis and the horizontal; ξ, a shape coefficient for a capillary (for a cylinder $\xi = 2$); σ, surface-tension coefficient; θ, wetting angle; r_p, radius of the pores; r_{opt}, optimal pore radius; a, coefficient for proportionality of permeability; Π, porosity; l, latent heat of vaporization; Q, heat flux; ρ, η', C_p', λ', density, viscosity, specific heat, and thermal conductivity of the liquid; ρ'', η'', density and viscosity of the vapor; Λ, resistance coefficient, $\Lambda = 0.066$; λ_e, effective thermal conductivity of the wick saturated with liquid; t, current temperature; r, coordinate; P, pressure; V, pore volume; K_m, dynamic permeability at a given pore radius r_{pm}.

LITERATURE CITED

1. Yu. F. Gerasimov et al., Inzh.-Fiz. Zh., 28, No. 6 (1975).
2. Yu. F. Gerasimov et al., Inzh.-Fiz. Zh., 30, No. 4 (1976).
3. Yu. A. Chizmadzhev et al., Macrokinetics of Porous Media Processes [in Russian], Nauka, Moscow (1972).
4. M. D. Mikhailov, Inzh.-Fiz. Zh., 11, No. 2 (1966).